Low-temperature thermochronology of the Izu collision zone, central Japan: Implications for mountain building at an active arc-arc collision zone

Sueoka, S.[1,*], Kobayashi, Y.[2], Fukuda, S.[1], Kohn, B.P.[3], Yokoyama, T.[1], Sano, N.[1], Hasebe, N.[4], Tamura, A.[4], Morishita, M.[4], Tagami, T.[2]

1: Japan Atomic Energy Agency, 2: Kyoto Univ., 3: Melbourne Univ., 4: Kanazawa Univ.
*sueoka.shigeru@jaea.go.jp

Key points

- Low-temperature thermochronology in an active arc-arc collision zone
- Rapid cooling/exhumation events coeval with collision event and plate motion change
- Mountain formation controlled by collision events and plate motions

1. Introduction & setting

The Izu collision zone has been an active arc-arc collision zone between Japanese Islands (i.e., NE and SW Japan Arcs) and Izu-Bonin Arc since the middle Miocene (Fig. 1a). Up to four collision events of crustal blocks of the Izu-Bonin Arc occured in the zone, i.e., by Kushigatayama Block at ~13 Ma, Misaka Block at ~10 Ma, Tanzawa Block at ~5 Ma, and Izu Block at ~1 Ma (Fig. 1b)(e.g., Matsuda, 1978; Amano, 1991; Kano, 2002; Hirata+, 2010). We performed low-T thermochronometries to reveal the mountain formation processes and their relations to the collision evetns. Apatite FT and U-Th/He methods were performed to reconstruct the exhuamation histories at the uppermost crust, whereas zircon U-Pb method was used to determine the crystallization ages of the plutons (Table 1).

Table 1: Sample list and dating methods applied.

Sample code	Region	Lithology	Geologic unit (plutonic body)	Location (WGS84) Latitude [°N]	Longitude [°E]	Elevation [m asl]	Dating method AFT	AHe	ZU-Pb
SFM17-K01	Tenshu Mts.	Quartz diorite	Sanogawa Plutonic Mass	35.271719	138.49753	383			
SFM17-K03	Minobu Mts.	Quartz diorite	Ojirogawa Plutonic Mass	35.319489	138.42035	362	Y	Y	Y
SFM17-K05	Tenshu Mts.	Quartz diorite	Shimobe Intrusive Rocks	35.394439	138.51929	906			
SFM17-K06	Tenshu Mts.	Quartz diorite	Shimobe Intrusive Rocks	35.401381	138.50280	679			
SFM17-K07	Misaka Mts.	Quartz diorite	Ashikawa Plutonic Mass	35.551508	138.65641	769			
SFM17-K08	Misaka Mts.	Quartz diorite	Ashikawa Plutonic Mass	35.549753	138.71189	1,134			
SFM17-K09.5	Misaka Mts.	Quartz diorite	Ashikawa Plutonic Mass	35.573922	138.74137	1,061			
SFM17-K11	Kanto Mts.	Granodiorite	Kofu Granodioritic Complex (Hirose pluton)	35.661469	138.80748	1,044	Y	Y	
SFM17-K12.5	Kanto Mts.	Granodiorite	Kofu Granodioritic Complex (Hirose pluton)	35.739753	138.81129	1,041	Y	Y	
SFM17-K15	Kanto Mts.	Granodiorite	Kofu Granodioritic Complex (Sanpo pluton)	35.857667	138.75877	1,108	Y	Y	Y
SFM17-K18	Kanto Mts.	Rhyolite	Chichibu Tonalite	36.028533	138.82926	1,154	Y	Y	
SFM17-K19	North Kanto	Granite	Namee Granite	36.231139	138.75777	327			
SFM17-K20	North Kanto	Granite	Namee Granite	36.242375	138.79194	377			
SFM17-K24	North Kanto	Granodiorite	Tsukuba Granite	36.213328	140.12621	295	Y	Y	
Sori06	North Kanto	Granodiorite	Sori Granodiorite	36.570147	139.39839	699	Y	Y	
SFM19-K03	Misaka Mts.	Quartz diorite	Ashikawa Plutonic Mass	35.557767	138.68054	981			
SFM19-K06	Misaka Mts.	Diorite	Dike	35.556583	138.78442	1,311			
SFM19-K08	Misaka Mts.	Granodiorite	Kofu Granodioritic Complex (Sasago pulton)	35.615206	138.77719	1,027	Y		
SFM19-K10	Kanto Mts.	Granodiorite	Oomiyama Granitoid	36.001192	138.56411	1,422	Y		

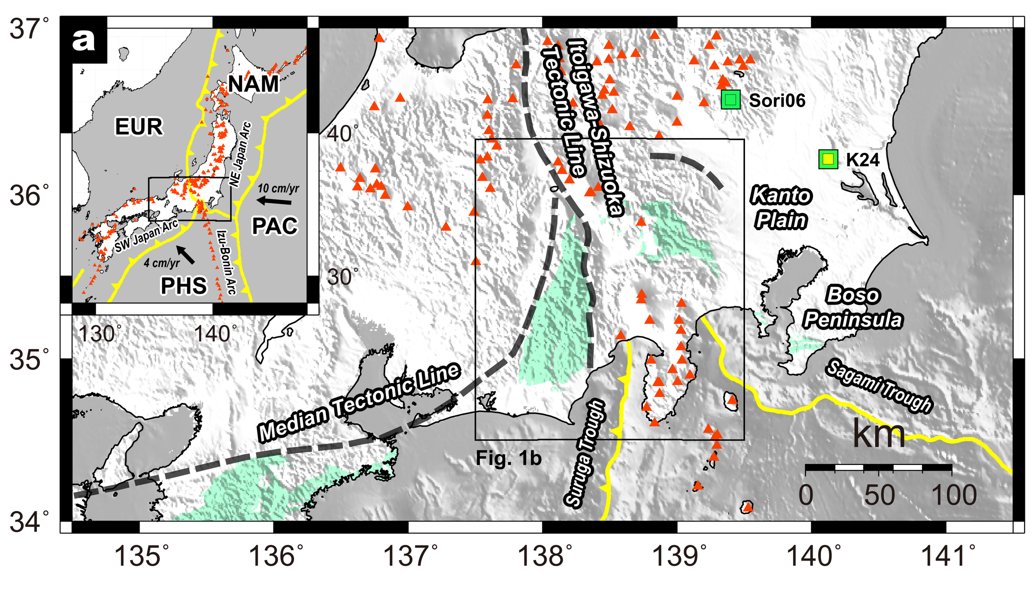

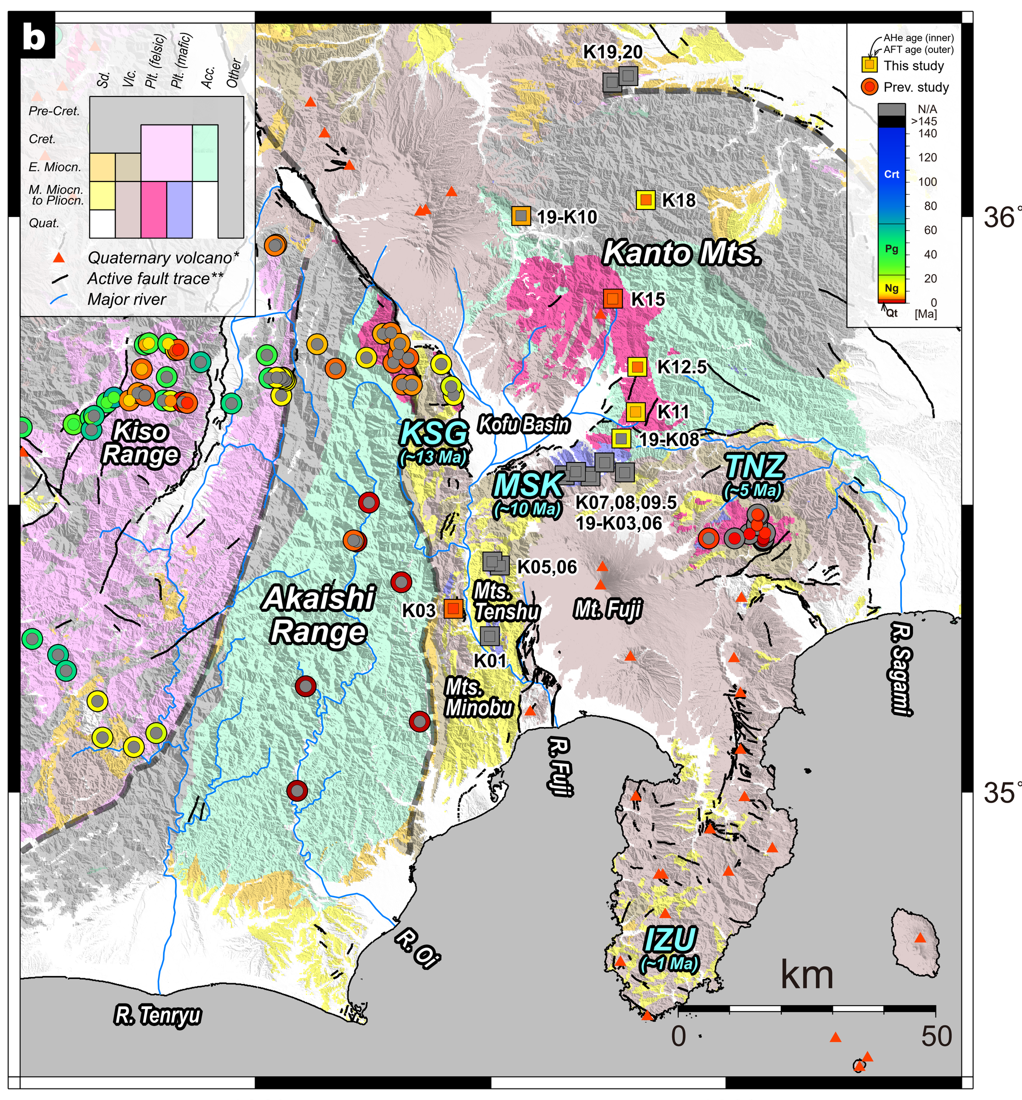

Figure 1: Index maps of study area. (a) Tectonic map in and around the Fossa Magna region. (b) Geologic map of the South Fossa Magna region (simplified after Wakita et al., 2009). The sampling localities in this study are indicated by the double squares, and those in previous studies are marked by the double circles (see Sueoka and Tagami, 2019 and references therein); the colors of the inner and outer circles/squares denote the AHe and AFT ages, respectively. The crustal blocks of the Izu-Bonin Arc are designated by abbreviations, with the approximate age of the collision event in light blue. KSG: Kushigatayama Block, MSK: Misaka Block, TNZ: Tanzawa Block, IZU: Izu Block, Sd.: sediments or sedimentary rocks, Vlc.: volcanic rocks, Plt.: plutonic rocks, Acc.: accretionary complexes. *Committee for Catalog of Quaternary Volcanoes in Japan (1999), **Nakata and Imaizumi (2002). ***Sueoka and Tagami (2019).

2. T-chron analyses & results

Rapid cooling episodes in the last few Myr were identified inside the collision zone, i.e., in Minobu Mts. (SFM17-K03) and Kanto Mts. (K11, K12.5, K15, K18). In contrast, samples K24 and Sori06 outside the collision zone yielded gradual and constant cooling in the last few 10 Myr.

Table 2: Summary of apatite fission-track data.

Sample code	Grains all-in	(zero track)	N_s	ρ_s [10^6/cm^2]	U [ppm]	Age ± 1σ [Ma]	P(χ^2) [%]	Cl ± 1σ [wt%]	F ± 1σ [wt%]	Tracks	Length ± 1σ [μm]
Unknown											
SFM17-K03	8	(6)	2	0.0067	3.7	3.6 ± 2.5	29.3	1.00 ± 0.08	2.35 ± 0.31	10	9.3 ± 3.5
SFM17-K11	34	(1)	77	0.053	13.6	7.6 ± 0.9	57.1	0.81 ± 0.08	2.93 ± 0.31	41	12.8 ± 3.6
SFM17-K12.5	22	(5)	20	0.037	7.8	9.2 ± 2.2	93.1	0.97 ± 0.16	3.39 ± 0.38	12	9.1 ± 2.0
SFM17-K15	37	(3)	61	0.052	33.9	3.0 ± 0.5	67.3	0.66 ± 0.11	3.04 ± 0.34	19	10.9 ± 3.4
SFM17-K18	8	(1)	10	0.033	4.4	14.7 ± 4.7	87.8	2.82 ± 0.12	1.83 ± 0.15	8	10.7 ± 4.3
SFM17-K24	8	(0)	211	0.56	29.2	37.0 ± 5.9	30.5	0.020 ± 0.004	4.35 ± 0.36	77	11.7 ± 1.9
Sori06	27	(0)	291	0.19	8.4	44.1 ± 4.0	49.3	0.049 ± 0.015	3.88 ± 0.60	41	12.1 ± 2.1
SFM19-K08	19	(0)	24	0.089	10.5	16.4 ± 3.7	25.0	-	-	-	-
SFM19-K10	9	(0)	12	0.098	36.1	5.3 ± 1.6	20.1	-	-	-	-
Age standard (Durango apatite)											
Dur-N1-19	6	(0)	130	0.160	10.3	29.5 ± 2.6	27.5	-	-	-	-

(Age parameters: Grains through F ± 1σ; Length parameters: Tracks, Length ± 1σ.)

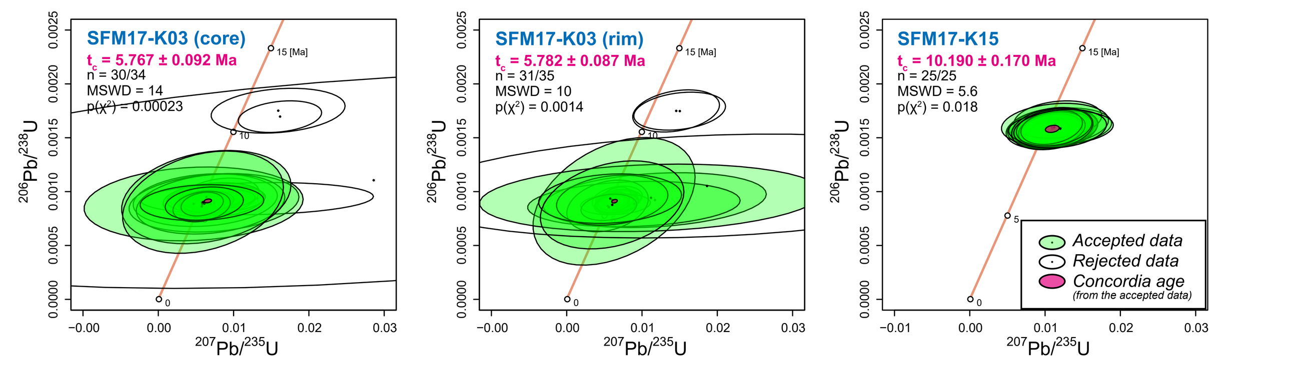

Figure 2: Concordia plots of zircon U–Pb data. The plots were drawn using IsoplotR (Vermeesch, 2018). The error ellipses present a range of ±95% Cl. t_c: Concordia age ±95% CI, n: number of accepted number of spots analyzed out of total number, MSWD: mean square of weighted deviates value for age homogeneity, p(χ^2): 95% of χ^2 distribution with one degree of freedom.

Figure 3: Charts of low-temperature thermochronologic data. (a) AHe grain age vs. eU. The error bars denote a range of ± 2σ. Data marked by crosses and orange error bars are outliers identified by IsoplotR (Vermeesch, 2018), which were excluded from the weighted mean calculation. The red lines indicate the range of the weighted mean AHe ages ±95% Cl. n: number of accepted grains per total number of dated grains, MSWD: mean square of weighted deviates value for age homogeneity, p(χ^2): 95% of χ^2 distribution with one degree of freedom . (b) AFT length histograms. The lengths are not projected onto the crystallographic c-axis. n: number of measured FTs, L: mean FT length ±1 standard deviation. (c) Thermal history inversion modeling results. The inverse calculations were performed using QTQt v. 5.8.0 (Gallagher, 2012) based on the AFT and AHe data.

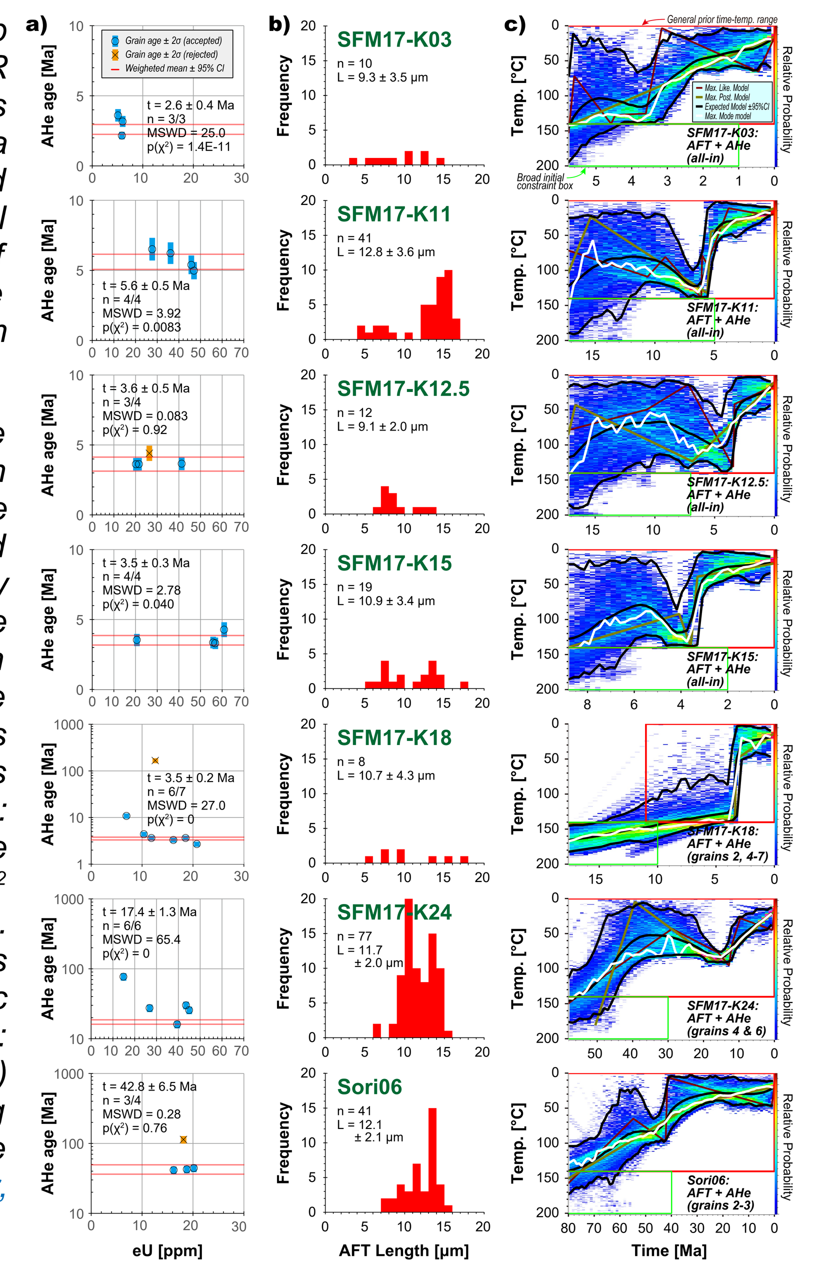

3. Tectonic/geologic implications

3-1. Uplift/denudation pattern of the Kanto Mountains

Timing of cooling gets younger to the center in the Kanto Mts (Fig. 3). This can be explained by assuming domal uplift rather than pop-up uplift (Fig. 4a). Domal uplift results in greater and later exhumation in the central part of the mountain, in contrast to pop-up uplift (Fig. 4b).

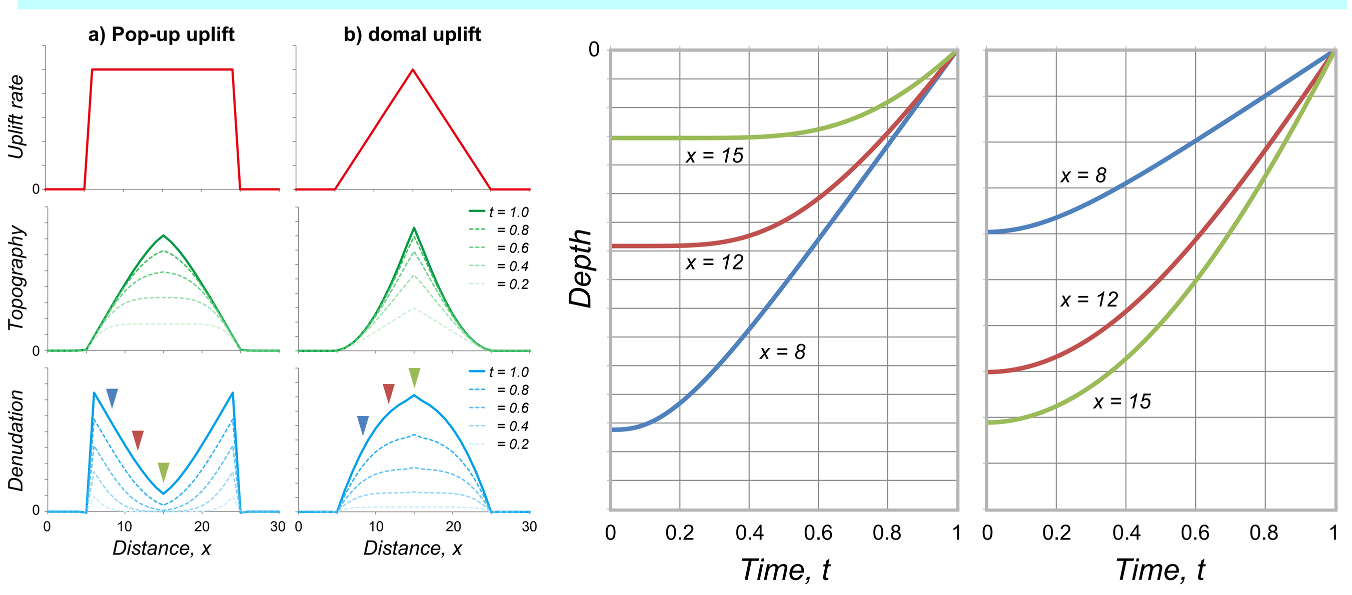

Figure 4: Modeled exhumation histories in two types of mountains. The temporal changes of topography and total amount of denudation are computed using two types of uplift patterns and the 2D mathematical model of slope development by Hirano (1972), which is based on the convection-diffusion equation (see also Sueoka et al., 2012).

$$\frac{\partial h}{\partial t} = a\frac{\partial^2 h}{\partial x^2} - b\left|\frac{\partial h}{\partial x}\right| + u(x,t)$$

where x is the distance, h is the elevation, t is the time, u is the bedrock uplift rate, and a and b are positive constants known as subduing coefficient and recessional coefficient, respectively. Note that the parameters are normalized. The lower plots show time-depth curves, i.e., exhumation histories, of rocks exposed at the surface at t = 1.0. The plots are obtained at x = 8, 12, and 15, as shown by the inverted triangles in the distance-denudation plots.

3-2. Tectonic histories of the Izu collision zone (synthesis)

Middle-late Miocene: collisions of KSG and MSK blocks; northward warping of the Izu collision zone (Kano, 2002); clockwise rotation of Kanto Mts. (Takahashi & Saito, 1997).

Early Pliocene: collision of TNZ block; domal uplift of Kanto Mts. (this study)

Late Pliocene: motional change of PHS plate from N to NW; initiation of E-W compression in the Japanese Islands (Takahashi, 2006); southward migration of the plate boundary (Hirata+2010); uplift of N-Akaishi Range by faulting of ISTL (Sueoka+2017); uplift of Minobu Mts. (this study)

Quaternary: collision of IZU block; uplift of S-Akaishi Range?? (Sueoka+2017)

Horizontal deformation predominated during the earlier stage of the arc-arc collision, but vertical movements developed at a later stage. This might indicate that the horizontal shortening and thickening of the crust and the resulting buoyancy play an important role in the vertical movements in the arc-arc collision zone.

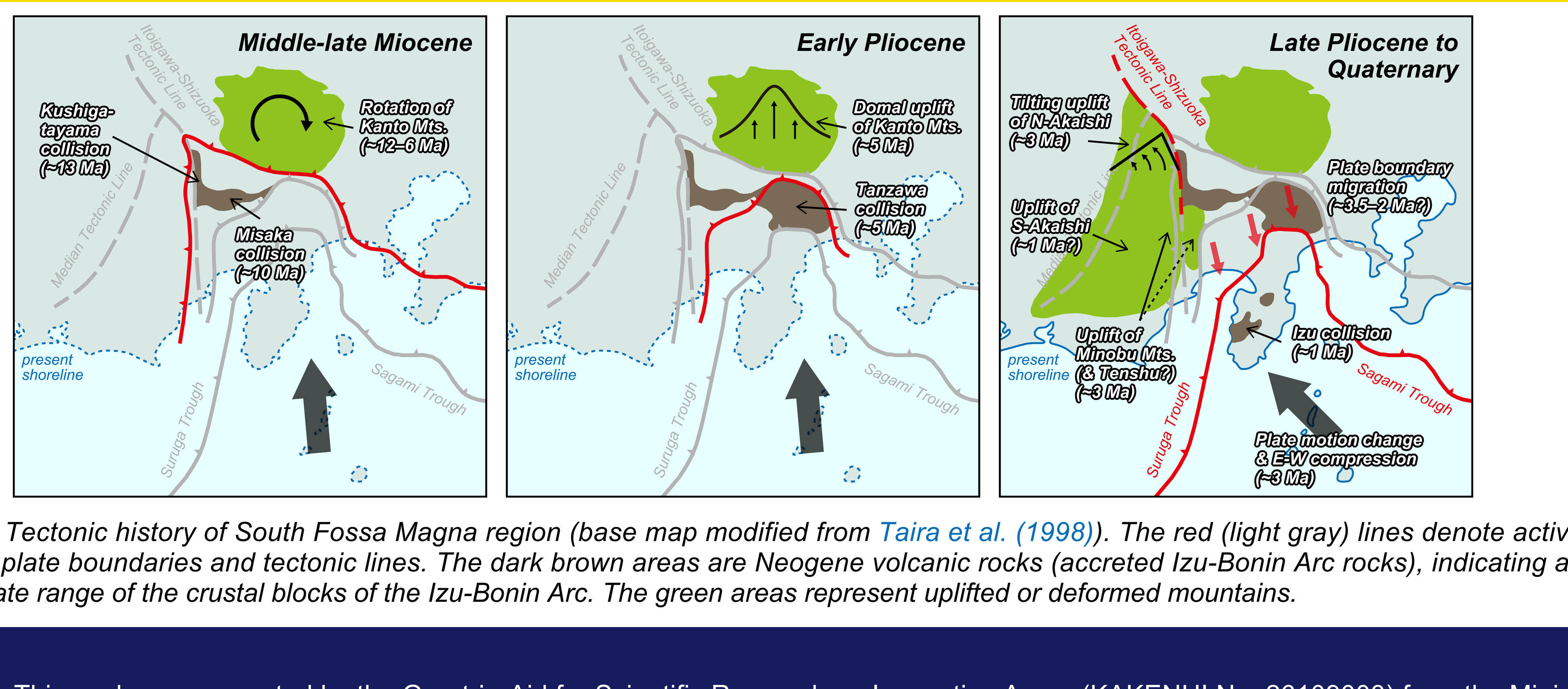

Figure 5: Tectonic history of South Fossa Magna region (base map modified from Taira et al. (1998)). The red (light gray) lines denote active (inactive) plate boundaries and tectonic lines. The dark brown areas are Neogene volcanic rocks (accreted Izu-Bonin Arc rocks), indicating an approximate range of the crustal blocks of the Izu-Bonin Arc. The green areas represent uplifted or deformed mountains.

Acknowledgement:

This manuscript was reorganized from part of the MSc thesis of author (YK) with additional investigations. This work was supported by the Grant-in-Aid for Scientific Research on Innovative Areas (KAKENHI No. 26109003) from the Ministry of Education, Culture, Sports, Science and Technology (MEXT). Sample Sori06 was offered by Dr. Masatsugu Ogasawara (the National Institute of Advanced Industrial Science and Technology; AIST). Sample collection and parts of the analyses were helped by Ai Shishikura, Yuya Kajita, and Saki Minami (Kyoto University). Mineral separations were carried out by Drs. Tohru Danhara and Hideki Iwano (Kyoto Fission-Track Co., Ltd). The Kanto Regional Environment Office permitted to collect rocks in the Chichibu-Tama-Kai and Fuji-Hakone-Izu National Parks. Ibaraki Prefecture permitted to collect rocks in the Suigo-Tsukuba Quasi-National Park. Some figures are drawn using the Generic Mapping Tools (GMT; Wessel and Smith, 1991), 50-m mesh DEM and GSI Map of the Geospatial Information Authority of Japan (GSI), and the GEBCO_08 Grid of the General Bathymetric Chart of the Oceans (GEBCO). The University of Melbourne thermochronology laboratory receives infrastructure support under the AuScope program of the National Collaborative Research Infrastructure Strategy (NCRIS).